UNSTEADY FREE CONVECTION HEAT AND MASS TRANSFER IN A WALTERS-B VISCOELASTIC FLOW PAST A SEMI-INFINITE VERTICAL PLATE: A NUMERICAL STUDY

by

Vallampati R. PRASAD [a*], *Buddakkagari VASU* [a],
Osman ANWAR BEG [b], *and Rana PARSHAD* [c]

[a] Department of Mathematics, Madanapalle Institute of Technology and Science,
Madanapalle, India
[b] Biomechanics, Biotechnology and Magnetohydrodynamics Research, Mechanical Engineering,
Program, Department of Engineering and Mathematics, Sheffield Hallam University, Sheffield,
England, UK
[c] Division of Mathematics and Computer Science, Clarkson University, New York, USA

A numerical solution for the free convective, unsteady, laminar convective heat and mass transfer in a viscoelastic fluid along a semi-infinite vertical plate is presented. The Walters-B liquid model is employed to simulate medical creams and other rheological liquids encountered in biotechnology and chemical engineering. This rheological model introduces supplementary terms into the momentum conservation equation. The dimensionless unsteady, coupled, and non-linear partial differential conservation equations for the boundary layer regime are solved by an efficient, accurate and unconditionally stable finite difference scheme of the Crank-Nicolson type. The velocity, temperature, and concentration fields have been studied for the effect of Prandtl number, viscoelasticity parameter, Schmidt number, and buoyancy ratio parameter. The local skin-friction, Nusselt number and Sherwood number are also presented and analyzed graphically. It is observed that, when the viscoelasticity parameter increases, the velocity increases close to the plate surface. An increase in Schmidt number is observed to significantly decrease both velocity and concentration.

Key words: *unsteady viscoelastic flow, semi-infinite vertical plate, Walters-B short-memory mode, finite difference method, mass transfer, Schmidt number*

Introduction

Heat and mass transfer in non-Newtonian fluids is of great interest in many operations in the chemical and process engineering industries including coaxial mixers [1], blood oxygenators [2], milk processing [3], steady-state tubular reactors, and capillary column

---

inverse gas chromatography devices [4], mixing mechanisms [5], bubble-drop formation processes [6], dissolution processes [7], and cloud transport phenomena [8]. Many liquids possess complex shear-stress relationships which deviate significantly from the Newtonian (Navier-Stokes) model. External thermal convection flows in such fluids have been studied extensively using mathematical and numerical models and often employ boundary-layer theory. Many geometrical configurations have been addressed including flat plates, channels, cones, spheres, wedges, inclined planes, and wavy surfaces. Non-Newtonian heat transfer studies have included power-law fluid models [9-11] *i. e.* shear-thinning and shear thickening fluids, simple viscoelastic fluids [12, 13], Criminale-Ericksen-Fibley viscoelastic fluids [14], Johnson-Segalman rheological fluids [15], Bingham yield stress fluids [16], second grade (Reiner-Rivlin) viscoselastic fluids [17], third grade viscoelastic fluids [18], micropolar fluids [19], and bi-viscosity rheological fluids [20]. Viscoelastic properties can enhance or depress heat transfer rates, depending upon the kinematic characteristics of the flow field under consideration and the direction of heat transfer [21]. The Walters-B viscoelastic model [21] was developed to simulate viscous fluids possessing short memory elastic effects and can simulate accurately many complex polymeric, biotechnological, and tribological fluids. The Walters-B model has therefore been studied extensively in many flow problems. Soundalegkar and Puri [22] presented one of the first mathematical investigations for such a fluid considering the oscillatory two-dimensional viscoelastic flow along an infinite porous wall, showing that an increase in the Walters elasticity parameter and the frequency parameter reduces the phase of the skin-friction. Rath *et al.* [23] used a perturbation method to analyze the steady flow and heat transfer of Walters-B model viscoelastic liquid between two parallel uniformly porous disks rotating about a common axis, showing that drag is enhanced with suction but reduced with injection and that heat transfer rate is accentuated with a rise in wall suction or injection. Roy *et al.* [24] investigated heat transfer in Walters-B viscoelastic flow along a plane wall with periodic suction using a perturbation method including viscous dissipation effects. Raptis *et al.* [25] studied flat plate thermal convection boundary layer flow of a Walters-B fluid using numerical shooting quadrature. Chang *et al.* [26] analyzed the unsteady buoyancy-driven flow and species diffusion in a Walters-B viscoelastic flow along a vertical plate with transpiration effects. They showed that the flow is accelerated with a rise in viscoelasticity parameter with both time and distances close to the plate surface and that increasing Schmidt number suppresses both velocity and concentration in time whereas increasing species Grashof number (buoyancy parameter) accelerates flow through time. Nanousis [27] used a Laplace transform method to study the transient rotating hydromagnetic Walters-B viscoelastic flow regime. Hydrodynamic stability studies of Walters-B viscoelastic fluids were communicated by Sharma *et al.* [28] for the rotating porous media suspension regime and by Sharma *et al.* [29] for Rayleigh-Taylor flow in a porous medium. Chaudhary *et al.* [30] studied the Hall current and cross-flow effects on free and forced Walters-B viscoelastic convection flow with thermal radiative flux effects. Mahapatra *et al.* [31] examined the steady two-dimensional stagnation-point flow of a Walters-B fluid along a flat deformable stretching surface. They found that a boundary layer is generated formed when the inviscid free-stream velocity exceeds the stretching velocity of the surface and the flow is accelerated with increasing magnetic field. This study also identified the presence of an inverted boundary layer when the surface stretching velocity exceeds the velocity of the free stream and showed that for this scenario the flow is decelerated with increasing magnetic field. Veena *et al.* [32] employed a perturbation and series expansion method and Kummer's functions to study two cases – prescribed power law surface temperature and prescribed

Prasad, V. R., *et al.*: Unsteady Free Convection Heat and Mass Transfer in a ...
THERMAL SCIENCE, Year 2011, Vol. 15, Suppl. 2, pp. S291-S305

S293

power law surface heat flux. They showed that an increase in viscoelasticity increases surface shear stresses. Rajagopal *et al.* [33] obtained exact solutions for the combined non-similar hydromagnetic flow, heat, and mass transfer phenomena in a conducting viscoelastic Walters--B fluid percolating a porous regime adjacent to a stretching sheet with heat generation, viscous dissipation and wall mass flux effects, using confluent hypergeometric functions for different thermal boundary conditions at the wall.

Steady free convection heat and mass transfer flow of an incompressible viscous fluid past an infinite or semi-infinite vertical plate is studied since long because of its technological importance. Pohlhausen [34], Somers [35], and Mathers *et al.* [36] were the first to study it for a flow past a semi-infinite vertical plate by different methods. But the first systematic study of mass transfer effects on free convection flow past a semi-infinite vertical plate was presented by Gebhart *et al.* [37] who presented a similarity solution to this problem and introduced a parameter *N* which is a measure of relative importance of chemical and thermal diffusion causing a density difference that drives the flow. Soundalgekar *et al.* [38] studied transient free convective flow past a semi-infinite vertical flat plate with mass transfer by using Crank-Nicolson finite difference method. In their analysis they observed that, an increase in *N* leads to an increase in the velocity but a decrease in the temperature and concentration. Prasad *et al.* [39] studied radiation effects on MHD unsteady free convection flow with mass transfer past a vertical plate with variable surface temperature and concentration. Owing to the significance of this problem in chemical and medical biotechnological processing (*e. g.* medical cream manufacture) we study the transient case of such a flow in the present paper using the robust Walters-B viscoelastic rheological material model. A Crank-Nicolson finite difference scheme is utilized to solve the unsteady dimensionless, transformed velocity, thermal and concentration boundary layer equations in the vicinity of the vertical plate. The present problem has to the author' knowledge not appeared thus far in the literature. Another motivation of the study is to further investigate the observed high heat transfer performance commonly attributed to extensional stresses in viscoelastic boundary layers [24]

Constitutive equations for the Walters-B viscoelastic fluid

Walters [21] has developed a physically accurate and mathematically amenable model for the rheological equation of state of a viscoelastic fluid of short memory. This model has been shown to capture the characteristics of actual viscoelastic polymer solutions, hydrocarbons, paints and other chemical engineering fluids. The Walters-B model generates highly non-linear flow equations which are an order higher than the classical Navier-Stokes (Newtonian) equations. It also incorporates elastic properties of the fluid which are important in extensional behaviour of polymers. The constitute equations for a Walters-B liquid in tensorial form may be presented as follows:

$$p_{ik} = -pg_{ik} + p_{ik}^{*} \tag{1}$$

$$p_{ik}^{*} = 2\int_{-\infty}^{t} \Psi(t - t^{*})e_{ik}^{(1)}(t^{*})\mathrm{d}t^{*} \tag{2}$$

$$\Psi(t - t^{*}) = \int_{0}^{\infty} \frac{N(\tau)}{\tau} e^{[-(t-t^{*})/\tau]}\mathrm{d}\tau \tag{3}$$

S294

Prasad, V. R., *et al.*: Unsteady Free Convection Heat and Mass Transfer in a ...
THERMAL SCIENCE, Year 2011, Vol. 15, No. 2, pp. S291-S305

where p_{ik} is the stress tensor, p – the arbitrary isotropic pressure, g_{tk} – the metric tensor of a fixed co-ordinate system x_i, $e_{ik}^{(1)}$ – the rate of strain tensor, and $N(\tau)$ – the distribution function of relaxation times, τ. The following generalized form of eq. (2) has been shown by Walters [21] to be valid for all classes of motion and stress:

$$p^{*ik}(x,t) = 2 \int_{-\infty}^{t} \Psi(t-t^*) \frac{\partial x^i}{\partial x^{*m}} \frac{\partial x^k}{\partial x^{*r}} e^{(1)mr}(x^* t^*) \mathrm{d}t^* \tag{4}$$

in which $x_i^* = x_i^*(x,t,t^*)$ denotes the position at time t^* of the element which is instantaneously at the position, x_i, at time, t. Liquids obeying the relations (1) and (4) are of the Walters-B' type. For such fluids with short memory *i. e.* low relaxation times, eq. (4) may be simplified to:

$$p^{*ik}(x,t) = 2\eta_0 e^{(1)ik} - 2k_0 \frac{\partial e^{(1)ik}}{\partial t} \tag{5}$$

in which $\eta_0 = \int_0^\infty N(\tau)\mathrm{d}\tau$ defines the limiting Walters-B' viscosity at low shear rates, $k_0 = \int_0^\infty \tau N(\tau)\mathrm{d}\tau$ is the Walters-B' viscoelasticity parameter and $\partial/\partial t$ is the convected time derivative. This rheological model is very versatile and robust and provides a relatively simple mathematical formulation which is easily incorporated into boundary layer theory for engineering applications [24, 25].
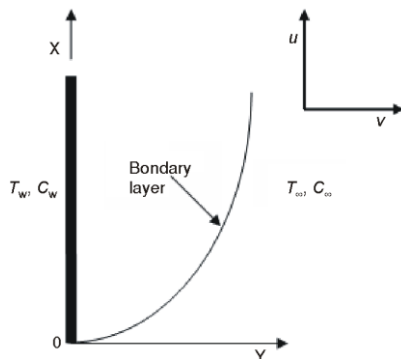
Mathematical model

Figure 1(a). Flow configuration and co-ordinate system

An unsteady 2-D laminar free convective flow of a viscoelastic fluid past a semi-infinite vertical plate is considered. The x-axis is taken along the plate in the upward direction and the y-axis is taken normal to it. The physical model is shown in fig. 1(a).

Initially, it is assumed that the plate and the fluid are at the same temperature T'_∞ and concentration level C'_∞ everywhere in the fluid. At time $t' > 0$, Also, the temperature of the plate and the concentration level near the plate are raised to T'_w and C'_w, respectively, and are maintained constantly thereafter. It is assumed that the concentration C' of the diffusing species in the binary mixture is very less in comparison to the other chemical species, which are present, and hence the Soret and Dufour effects are negligible. It is also assumed that there is no chemical reaction between the diffusing species and the fluid. Then, under the above assumptions, the governing boundary layer equations with Boussinesq's approximation are:

$$\frac{\partial u}{\partial x} + \frac{\partial v}{\partial y} = 0 \tag{6}$$

$$\frac{\partial u}{\partial t'} + u\frac{\partial u}{\partial x} + v\frac{\partial u}{\partial y} = g\beta(T'-T'_\infty) + g\beta^*(C'-C'_\infty) + v\frac{\partial^2 u}{\partial y^2} - k_0\frac{\partial^3 u}{\partial y^2 \partial t'} \tag{7}$$

Prasad, V. R., *et al.*: Unsteady Free Convection Heat and Mass Transfer in a …
THERMAL SCIENCE, Year 2011, Vol. 15, Suppl. 2, pp. S291-S305

S295

$$\frac{\partial T'}{\partial t'} + u\frac{\partial T'}{\partial x} + v\frac{\partial T'}{\partial y} = \alpha\frac{\partial^2 T'}{\partial y^2} \tag{8}$$

$$\frac{\partial C'}{\partial t'} + u\frac{\partial C'}{\partial x} + v\frac{\partial C'}{\partial y} = D\frac{\partial^2 C'}{\partial y^2} \tag{9}$$

The initial and boundary conditions are:

$$
\begin{aligned}
t' \leq 0: \quad & u=0, \ v=0, \quad T'=T'_\infty, \quad C'=C'_\infty \\
t' > 0: \quad & u=0, \ v=0, \quad T'=T'_w, \quad C'=C'_w \quad \text{at} \ y=0 \\
& u=0, \quad T'=T'_\infty, \quad C'=C'_\infty \quad \text{at} \ x=0 \\
& u \to 0, \ T' \to T'_\infty, \ C' \to C'_\infty \quad \text{as} \ y \to \infty
\end{aligned}
\tag{10}
$$

where u and v are velocity components in x- and y-directions, respectively, t' is the time, g – the acceleration due to gravity, β – the volumetric coefficient of thermal expansion, β^*– the volumetric coefficient of expansion with concentration, T' – the temperature of the fluid in the boundary layer, C'– the species concentration in the boundary layer, T'_w - the wall temperature, T'_∞ – the free stream temperature far away from the plate, C'_w – the concentration at the plate, C'_∞ – the free stream concentration in fluid far away from the plate, v – the kinematic viscosity, α – the thermal diffusivity, ρ – the density of the fluid, and D – the species diffusion coefficient.

On introducing the following non-dimensional quantities:

$$X=\frac{x}{L}, \quad Y=\frac{y\,\mathrm{Gr}^{1/4}}{L}, \quad U=\frac{uL\,\mathrm{Gr}^{-1/2}}{v}, \quad V=\frac{vL\,\mathrm{Gr}^{-1/4}}{v}, \quad \theta=\frac{T'-T'_\infty}{T'_w-T'_\infty}, \quad C=\frac{C'-C'_\infty}{C'_w-C'_\infty}$$

$$t'=\frac{tL^2}{v}\mathrm{Gr}^{-1/2}, \quad N=\frac{\beta^*(C'_w-C'_\infty)}{\beta(T'_w-T'_\infty)}, \quad \mathrm{Gr}=\frac{L^3 g\beta(T'_w-T'_\infty)}{v^2},$$

$$\Gamma=\frac{k_0\sqrt{\mathrm{Gr}}}{L^2}, \quad \mathrm{Pr}=\frac{v}{\alpha}, \quad \text{and} \ \mathrm{Sc}=\frac{v}{D} \tag{11}$$

Equations (6) to (10) are reduced to the following non-dimensional form:

$$\frac{\partial U}{\partial X} + \frac{\partial V}{\partial Y} = 0 \tag{12}$$

$$\frac{\partial U}{\partial t} + U\frac{\partial U}{\partial X} + V\frac{\partial U}{\partial Y} = \frac{\partial^2 U}{\partial Y^2} + T + NC - \Gamma\frac{\partial^3 U}{\partial Y^2 \partial t} \tag{13}$$

$$\frac{\partial T}{\partial t} + U\frac{\partial T}{\partial X} + V\frac{\partial T}{\partial Y} = \frac{1}{\mathrm{Pr}}\frac{\partial^2 T}{\partial Y^2} \tag{14}$$

$$\frac{\partial C}{\partial t} + U\frac{\partial C}{\partial X} + V\frac{\partial C}{\partial Y} = \frac{1}{\mathrm{Sc}}\frac{\partial^2 C}{\partial Y^2} \tag{15}$$

S296

Prasad, V. R., *et al.*: Unsteady Free Convection Heat and Mass Transfer in a ...
THERMAL SCIENCE, Year 2011, Vol. 15, No. 2, pp. S291-S305

The corresponding initial and boundary conditions are:

$$
\begin{aligned}
t \le 0: \quad & U = 0, \quad V = 0, \quad T = 0, \quad C = 0, \\
t > 0: \quad & U = 0, \quad V = 0, \quad T = 1, \quad C = 1 \quad \text{at} \quad Y = 0 \\
& U = 0, \quad T = 0, \quad C = 0 \qquad\qquad \text{at} \quad X = 0 \\
& U \to 0, \quad T \to 0, \quad C \to 0 \qquad \text{as} \quad Y \to \infty
\end{aligned}
\tag{16}
$$

where Gr is the thermal Grashof number, Pr − the fluid Prandtl number, Sc − the Schmidt number, and N − the buoyancy ratio parameter.

To obtain an estimate of flow dynamics at the barrier boundary, we also define several important rate functions at $Y = 0$. These are the dimensionless wall shear stress function, *i. e.* local skin friction function, the local Nusselt number (dimensionless temperature gradient) and the local Sherwood number (dimensionless species, *i. e.* contaminant transfer gradient) are computed with the following mathematical expressions [40]:

$$
\tau_X = \sqrt[4]{Gr^3}\left(\frac{\partial U}{\partial Y}\right)_{Y=0}, \quad
Nu_X = \frac{-X\sqrt[4]{Gr}\left(\dfrac{\partial T}{\partial Y}\right)_{Y=0}}{T_{Y=0}}, \quad
Sh_X = \frac{-X\sqrt[4]{Gr}\left(\dfrac{\partial C}{\partial Y}\right)_{Y=0}}{C_{Y=0}}
\tag{17}
$$

We note that the dimensionless model defined by eqs. (12) to (15) under conditions (16) reduces to Newtonian flow in the case of vanishing viscoelasticity *i. e.* when $\Gamma \to 0$.

Numerical solution

In order to solve these unsteady, non-linear coupled equations (12) to (15) under the conditions (16), an implicit finite difference scheme of Crank-Nicolson type has been employed. This method was originally developed for heat conduction problems [41]. Prasad *et al.* [42] described the solution procedure in detail. The region of integration is considered as a rectangle with $X_{max.} = 1$ and $Y_{max.} = 14$ where $Y_{max.}$ corresponds to $Y = \infty$ which lies well outside the momentum, thermal, and concentration boundary layers. After some preliminary numerical experiments the mesh sizes have been fixed as $\Delta X = 0.05$, $\Delta Y = 0.25$ with time step $\Delta t = 0.01$. The computations are executed initially by reducing the spatial mesh sizes by 50% in one direction, and later in both directions by 50% and the results are compared. It is observed that, in all the cases, the results differ only in the fifth decimal place. Hence these mesh sizes are considered to be appropriate mesh sizes for present calculations. The local truncation error in the finite difference approximation is $O(\Delta t^2 + \Delta X + \Delta Y^2)$ and it tends to zero as Δt, ΔX, and ΔY tend to zero. Hence the scheme is compatible. The scheme is unconditionally stable as explained by Prasad *et al.* [42]. Stability and compatibility ensures convergence.

Results and discussion

In order to ascertain the accuracy of the numerical results, the present study is compared with the previous study. The velocity profiles for Sc = 0.3 and 0.6, Pr = 0.73, $N = 2.0$, $\Gamma = 0.0$ at $X = 1.0$ are compared with the available solution of Soundalgekar *et al.* [38] in fig. 1. It is observed that the present results are in good agreement with that of Soundalgekar *et al.* [38].

Prasad, V. R., *et al.*: Unsteady Free Convection Heat and Mass Transfer in a …
THERMAL SCIENCE, Year 2011, Vol. 15, Suppl. 2, pp. S291-S305

S297

Only selective figures have been repro-
duced here for brevity. Default values of the
parameters are: viscoelasticity parameter (Γ) =
= 0.005, buoyancy ratio parameter (N) = 1.0,
Schmidt number (Sc) = 0.6 (oxygen diffusing
in the viscoelastic fluid), and Prandtl number
(Pr) = 0.71 (water-based solvents). All
graphs therefore correspond to these values
unless specifically otherwise indicated. For
the special case of Sc = 1, the species
diffuses at the same rate as momentum in the
viscoelastic fluid. Both concentration and
boundary layer thicknesses are the same for
this case. For Sc < 1, species diffusivity
exceeds momentum diffusivity, so that mass
is diffused faster than momentum. The

Figure 1(b). Comparison of velocity profiles at
$X = 1.0$

opposite case applies when Sc > 1. An increase in Sc will suppress concentration in the
boundary layer regime since higher Sc values will physically manifest in a decrease of
molecular diffusivity (D) of the viscoelastic fluid *i. e.* a reduction in the rate of mass diffusion.
Lower Sc values will exert the reverse influence since they correspond to higher molecular
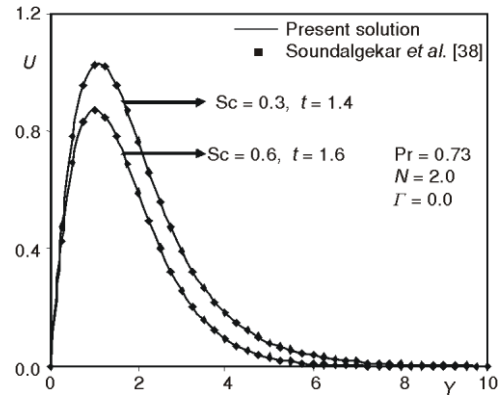diffusivities. Concentration boundary layer thickness is generally greater for Sc < 1 than for
Sc > I.

In figs. 2(a) to (c), we have presented the variation of velocity (U), temperature
function (T) and concentration (C) *vs*. (Y) with collective effects of viscoelasticity (Γ) at X =
= 1.0. An increase in Γ from 0 to 0.001, 0.003, and 0.005, and the maximum value of 0.007,
as depicted in fig. 2(a), clearly enhances the velocity U which ascends sharply and peaks in
close vicinity to the plate surface (Y = 0). With increasing distance from the plate wall
however the velocity U is adversely affected by increasing viscoelasticity *i. e.* the flow is
decelerated. Therefore close to the plate surface the flow velocity is maximized for the case of
a Newtonian fluid (vanishing viscoelastic effect *i. e.* Γ = 0) but this trend is reversed as we
progress further into the boundary layer regime. The switchover in behavior corresponds to
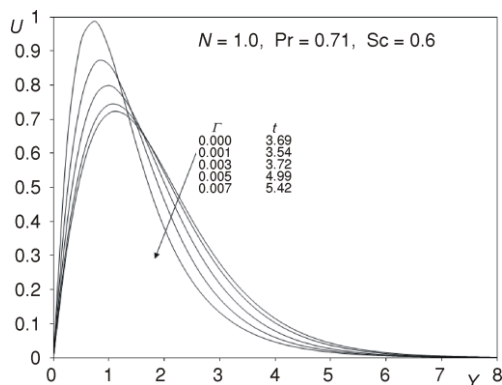

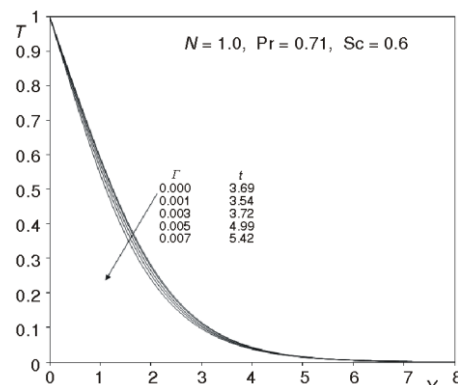**Figure 2(a). Steady-state velocity profiles at**
$X = 1.0$ for different Γ

Figure 2(b). Steady-state temperature profiles at
$X = 1.0$ for different Γ

S298

Prasad, V. R., *et al.*: Unsteady Free Convection Heat and Mass Transfer in a …
THERMAL SCIENCE, Year 2011, Vol. 15, No. 2, pp. S291-S305

approximately $Y = 1.5$. With increasing (Y) velocity profiles decay smoothly to zero in the free stream at the edge of the boundary layer. The opposite effect is caused by an increase in time. A rise in t from 3.69 through 3.54, 3.72, 4.98, to 5.42 causes a decrease in flow velocity U nearer the wall in this case the maximum velocity arises for the least time progressed. With more passage of time ($t = 5.42$) the flow is decelerated. Again there is a reverse in the response at $Y \sim 1$, and thereafter velocity is maximized with the greatest value of time. In fig. 2(b) increasing viscoelasticity Γ is seen to decrease temperature throughout the boundary layer. As we approach the free stream the effects of viscoelasticity are negligible since the profiles are all merged together. All profiles decay from the maximum at the wall to zero in the free stream. The graphs show therefore that increasing viscoelasticity cools the flow. With progression of time, however the temperature, T is consistently enhanced *i. e.* the fluid is heated as time progresses.

A similar response is observed for the concentration field, C, in fig. 2(c). Increasing viscoelasticity again reduces concentration, showing that species diffuses more effectively in Newtonian fluids ($\Gamma = 0$) than in strongly viscoelastic fluids. Once again with greater elapse in time the concentration values are reduced throughout the boundary layer regime ($0 < Y << 14$).
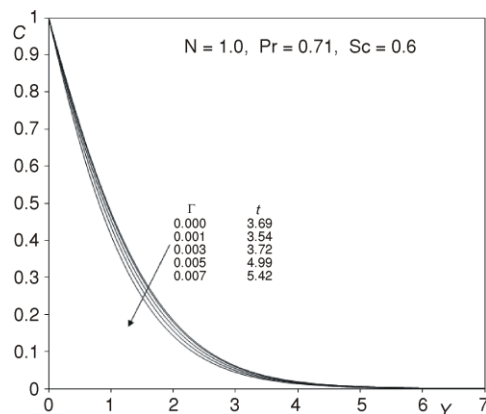

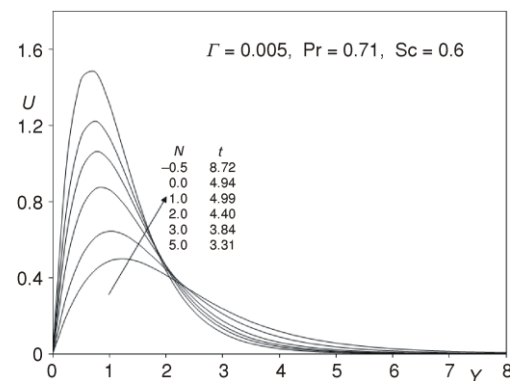**Figure 2(c). Steady-state concentration profiles at $X = 1.0$ for different Γ**

Figure 3(a). Steady-state velocity profiles at $X= 1.0$ for different N

Figures 3(a) to 3(c), present the effects of buoyancy ratio parameter N on U, T, and C profiles. The maximum time elapse to the steady-state scenario accompanies the only negative value of N *i. e.* $N = -0.5$. For $N = 0$ and then increasingly positive values of N up to 5.0, the time taken, t, is steadily reduced. As such the presence of aiding buoyancy forces (both thermal and species buoyancy force acting in unison) serves to stabilize the transient flow regime. The parameter $N = \beta^{*}(C_{w}' - C_{\infty}')/\beta(T_{w}' - T_{\infty}')$ and expresses the ratio of the species (mass diffusion) buoyancy force to the thermal (heat diffusion) buoyancy force. When $N = 0$ the species buoyancy term, NC vanishes and the momentum boundary layer eq. (13) is de-coupled from the species diffusion (concentration) boundary layer eq. (15). Thermal buoyancy does not vanish in the momentum eq. (13) since the term T is not affected by the buoyancy ratio. When $N < 0$ we have the case of opposing buoyancy. An increase in N from -0.5, through 0, 1, 2, 3, to 5 clearly accelerates the flow *i. e.* induces a strong escalation in streamwise velocity U, close to the wall; thereafter velocities decay to zero in the free stream. At some distance from the plate surface, approximately $Y = 2.0$, there is a cross-over in

Prasad, V. R., *et al.*: Unsteady Free Convection Heat and Mass Transfer in a …
THERMAL SCIENCE, Year 2011, Vol. 15, Suppl. 2, pp. S291-S305

S299

profiles. Prior to this location the above trends are apparent. However after this point, increasingly positive N values in fact decelerate the flow. Therefore further from the plate surface, negative N *i. e.* opposing buoyancy is beneficial to the flow regime whereas closer to the plate surface it has a retarding effect.
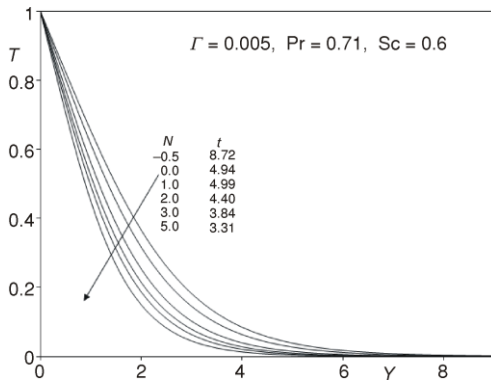

Figure 3(b). Steady-state temperature profiles at $X = 1.0$ for different N
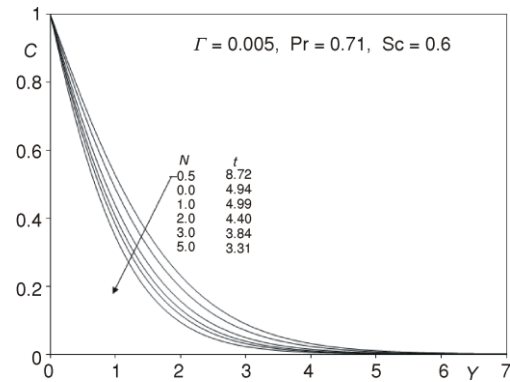
Figure 3(c) Steady-state concentration profiles at $X = 1.0$ for different N

A much more consistent response to a change in the N parameter is observed in fig. 3(b), where with a rise from –0.5 through 0, 1.0, 2.0, 3.0, to 5.0 (very strong aiding buoyancy case) the temperature throughout the boundary layer is strongly reduced. As with the velocity field fig. 3(a), the time required to attain the steady-state decreases substantially with a positive increase in N. Aiding (assisting) buoyancy therefore stabilizes the temperature distribution. A similar response is evident for the concentration distribution, C, which as shown in fig. 3(c), also decreases with positive increase in N but reaches the steady-state progressively faster.

Figures 4(a) to (c) illustrate the effect of Prandtl number and time t on velocity U, temperature T, and concentration C. Increasing Pr clearly reduces strongly velocity U, fig. 4(a), both in the near-wall regime and the far-field regime of the boundary layer.

Figure 4(a) Steady-state velocity profiles at $X = 1.0$ for different Pr
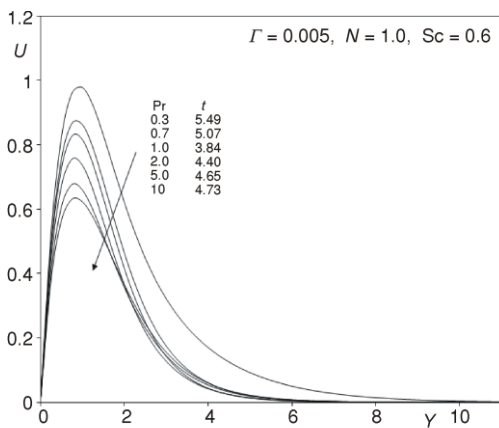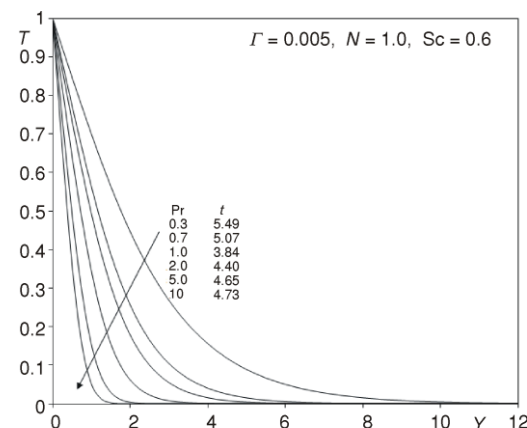
Figure 4(b) Steady-state temperature profiles at $X = 1.0$ for different Pr
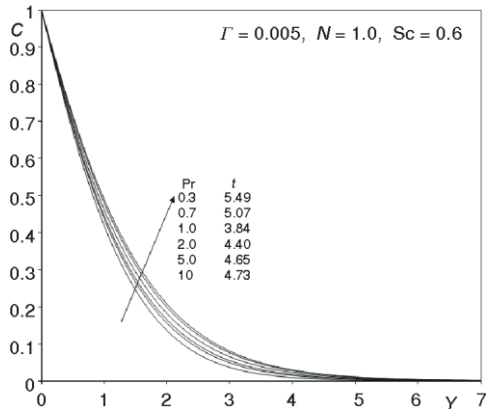
Figure 4(c) Steady-state concentration profiles at $X = 1.0$ for different Pr

Velocity is therefore maximized when Pr = = 0.3 (minimum) and minimized for the largest value of Pr (10.0). Pr defines the ratio of momentum diffusivity (v) to thermal diffusivity. Pr < 1 physically corresponds to cases where heat diffuses faster than momentum. Pr = 0.7 is representative of water-based solvents and Pr $\gg$ 1 *e. g.* 10 corresponds to lubricating oils, *etc*. An increase in time, *t*, also serves to strongly retard the flow. With increasing Pr from 0.3 through 0.7, 1.0, 5.0, to 10.0, temperature *T* as shown in fig. 5(b), is markedly reduced throughout the boundary layer. The descent is increasingly sharper near the plate surface for higher Pr values. With lower Pr values a more gradual (monotonic) decay is witnessed. Smaller Pr values in this case, cause a thinner thermal boundary layer thickness and more uniform temperature distributions across the boundary layer. Smaller Pr fluids possess higher thermal conductivities so that heat can diffuse away from the plate surface (wall) faster than for higher Pr fluids (thicker boundary layers). Our computations show that a rise in Pr depresses the temperature function, a result consistent with numerous other studies on coupled heat and mass transfer [43]. For the case of Pr = 1, thermal and velocity boundary layer thicknesses are equal.

Conversely the concentration values, fig. 4(c), are slightly increased with a rise in Pr from 0.3 through intermediate values to 10. However with progression of time the concentration is found to be decreased in the boundary layer regime.

Figures 5(a) and (b) depict the distributions of velocity (*U*) and concentration (*C*) *vs.* co-ordinate (*Y*) for various Schmidt numbers (Sc) and time (*t*), close to the leading edge at $X = 1.0$, are shown. These figures again correspond to a viscoelasticity parameter $\Gamma = 0.005$ *i. e.* weak elasticity and strongly viscous effects. An increase in Sc from 0.1 (low weight diffusing gas species) through 0.5 (oxygen diffusing) to 1.0 (denser hydrocarbon derivatives
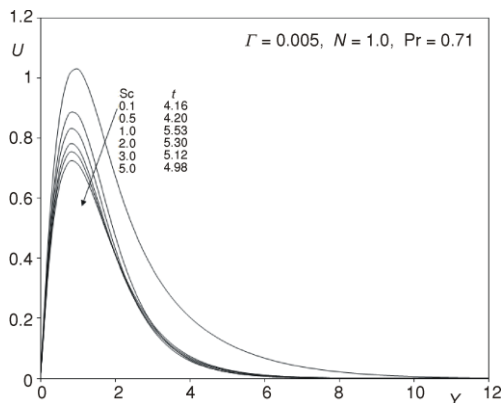

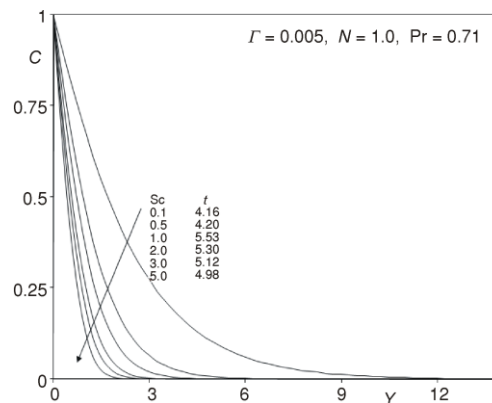**Figure 5(a). Steady-state velocity profiles at $X = 1.0$ for different Sc**

Figure 5(b). Steady-state concentration profiles at $X = 1.0$ for different Sc

as the diffusing species), 3.0 and 5.0, clearly strongly decelerates the flow. The maximum velocity arises at Sc = 0.1 very close to the wall. All profiles then descend smoothly to zero in the free stream. With higher Sc values the gradient of velocity profiles is lesser prior to the peak velocity but greater after the peak. An increase in time, t, is found to accelerate the flow. Figure 6(b) shows that a rise in Sc strongly suppresses concentration levels in the boundary layer regime. Sc defines the ratio of momentum diffusivity (ν) to molecular diffusivity (D). For Sc < 1, species will diffuse much faster than momentum so that maximum concentrations will be associated with this case (Sc = 0.1). For Sc > 1, momentum will diffuse faster than species causing progressively lower concentration values. All profiles decay monotonically from the plate surface (wall) to the free stream. With a decrease in molecular diffusivity (rise in Sc) concentration boundary layer thickness is therefore decreased. For the special case of Sc = 1, the species diffuses at the same rate as momentum in the viscoelastic fluid. Both concentration and boundary layer thicknesses are the same for this case. Concentration values are also seen to increase continuously with time, t. An increase in Schmidt number effectively depresses concentration values in the boundary layer regime since higher Sc values will physically manifest in a decrease of molecular diffusivity (D) of the viscoelastic fluid *i. e.* a reduction in the rate of mass diffusion. Lower Sc values will exert the reverse influence since they correspond to higher molecular diffusivities. Concentration boundary layer thickness is therefore considerably greater for Sc = 0.1 than for Sc = 5.

In figs. 6(a) to (c) the variation of dimensionless local skin friction (surface shear stress) τ_x, Nusselt number (surface heat transfer gradient) Nu_x, and the Sherwood number (surface concentration gradient) (Sh_x), *vs.* axial co-ordinate (X) for various viscoelasticity parameters (Γ) and time (t) are llustrated.
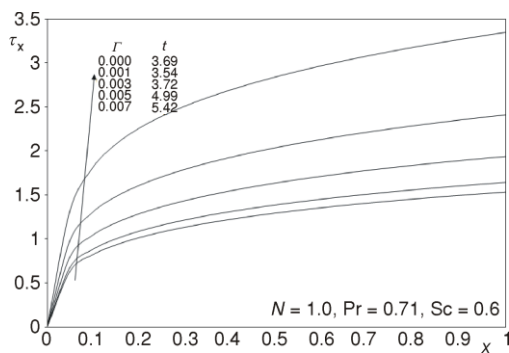
Figure 6(a). The local skin friction results for different Γ
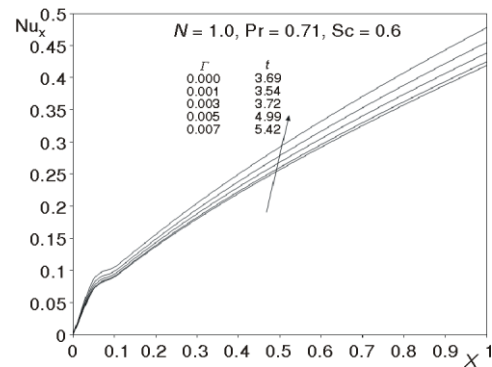
Figure 6(b). The local Nusselt number results for different Γ

Shear stress is clearly enhanced with increasing viscoelasticity (*i. e.* stronger elastic effects) *i. e.* the flow is accelerated, a trend consistent with our earlier computations in fig. 2(a). The ascent in shear stress is very rapid from the leading edge ($X = 0$) but more gradual as we progress along the plate surface away from the plane. With an increase in time, t, shear stress τ_x is however increased. Increasing viscoelasticity (Γ) is observed in fig. 6(b) to enhance local Nusselt number Nu_x, values whereas they are again increased with greater time. Similarly in fig. 6(c) the local Sherwood number Sh_x values are elevated with an increase in

S302

Prasad, V. R., *et al.*: Unsteady Free Convection Heat and Mass Transfer in a …
THERMAL SCIENCE, Year 2011, Vol. 15, No. 2, pp. S291-S305
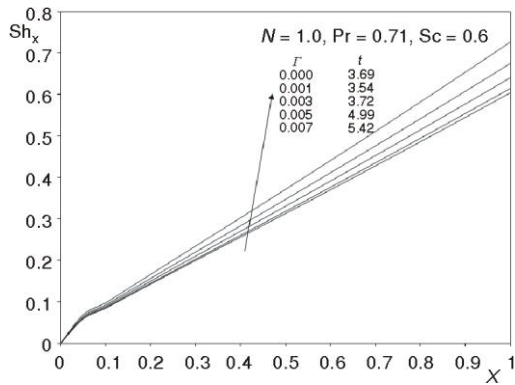
Figure 6(c). The local Shewood number results for different τ

elastic effects *i. e.* a rise in Γ from 0 (Newtonian flow) through 0.001, 0.003, 0.005 to 0.007 but depressed slightly with time.

Finally, in figs. 7(a) to (c) the influence of Sc and time t on τ_x, Nu_x, and Sh_x, *vs.* X, are depicted. An increase in Sc from 0.1 through 0.5, 1, 3 to 5, strongly reduces both τ_x and Nu_x along the entire plate surface *i. e.* for all X. However with an increase in t both shear stress and local Nusselt number are enhanced. With increasing Sc values, local Sherwood number Sh_x, as shown in fig. 7(c), is boosted considerably along the plate surface; gradients of the profiles are also found to diverge with increasing X values. However an increase in t, serves to reduce local Sherwood numbers.
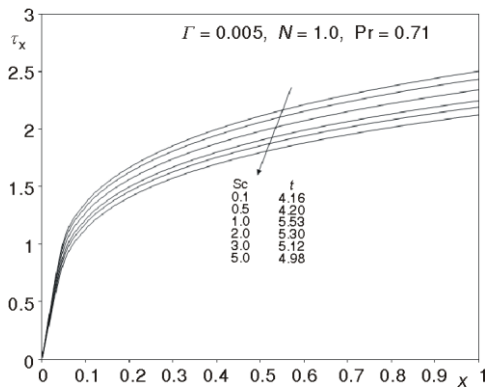
Figure 7(a). The local skin function results for different Sc
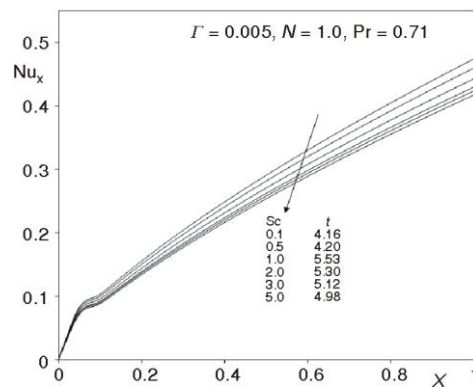
Figure 7(b). The local Nussult number results for different Sc

Figure 7(c). The local Sherwod number result for different Sc

Conclusions

A 2-D, unsteady laminar incompressible boundary layer model has been presented for the external flow, heat and mass transfer in a viscoelastic buoyancy-driven flow past a semi-infinite vertical plate. The Walters-B viscoelastic model has been employed which is valid for short memory polymeric fluids. The dimensionless conservation equations have been solved with the well-tested, robust, highly efficient, implicit Crank-Nicolson finite difference numerical method. The present

Prasad, V. R., *et al.*: Unsteady Free Convection Heat and Mass Transfer in a …
THERMAL SCIENCE, Year 2011, Vol. 15, Suppl. 2, pp. S291-S305

S303

computations have shown that increasing viscoelasticity accelerates the velocity and enhances shear stress (local skin friction), local Nusselt number and local Sherwood number, but reduces temperature and concentration in the boundary layer. Increasing viscoelasticity again reduces concentration, showing that species diffuses more effectively in Newtonian fluids (Γ = 0) than in strongly viscoelastic fluids. Owing to the significance of this problem in chemical and medical biotechnological processing (*e. g.* medical cream manufacture) we study the transient case of such a flow in the present paper using the robust Walters-B viscoelastic rheological material model. The present model has neglected thermal radiation effects. This phenomena is of interest in very high temperature (*e. g.* glass) flows in the mechanical and chemical process industries and is currently under investigation.

Nomenclature

C – dimensionless concentration
C' – concentration
D – mass diffusion coefficient
Gr – thermal Grashof number
g – gravitational acceleration
k_0 – Walters-B viscoelasticity parameter
L – reference length
N – buoyancy ration number
Nu_x – non-dimensional local Nusselt number
Pr – Prandtl number
Sc – Schmidt number
Sh_x – non-dimensional local Sherwood number
T – dimensionless temperature
T' – temperature
t – dimensionless time
t' – time
Δt – dimensionless time-step
U, V – dimensionless velocity components along the X- and Y-directions, respectively
u, v – velocity components along the x- and y-directions, respectively
X, Y – dimensionless spatial co-ordinates along the plate generator and normal to the generator, respectively

ΔX – dimensionless finite difference grid size in X-direction
ΔY – dimensionless finite difference grid size in Y-direction
x, y – co-ordinates along the plate generator and normal to the generator, respectively

Greek symbols

α – thermal diffusivity
β – volumetric thermal expansion coefficient
β^* – volumetric concentration expansion coefficient
Γ – viscoelastic parameter
ν – kinematic viscosity
τ_X – dimensionless local skin-friction

Subscripts

w – condition on the wall
∞ – free stream condition

References

[1] Thibault, F., Tanguy, P. A., Power-Draw Analysis of a Coaxial Mixer with Newtonian and Non-Newtonian Fluids in the Laminar Regime, *Chemical Engineering Science, 57* (2002), 18, pp. 3861-3872
[2] Goerke, A. R., Leung, J., Wickramasinghe, S. R., Mass and Momentum Transfer in Blood Oxygenators, *Chemical Engineering Science, 57* (2002), 11, pp. 2035-2046
[3] Wang, W., Chen, G., Heat and Mass Transfer Model of Dielectric-Material-Assisted Microwave Freeze-Drying of Skim Milk with Hygroscopic Effect, *Chemical Engineering Science, 60* (2005), 23, pp. 6542-6550
[4] Vrentas, J. S., Vrentas, C. M., Axial Moment Analyses of Convective Heat and Mass Transfer Processes, *Chemical Engineering Science, 51* (1996), 6, pp. 921-929
[5] Ayazi Shamlou, P., Edwards, M. F., Heat Transfer to Viscous Newtonian and Non-Newtonian Fluids for Helical Ribbon Mixers, *Chemical Engineering Science, 41* (1986), 8, pp. 1957-1967
[6] Jarzebski, A. B., Malinowski, J. J., Transient Mass and Heat Transfer from Drops or Bubbles in Slow Non-Newtonian Flows, *Chemical Engineering Science, 41* (1986), 10, pp. 2575-2578

[7]   Elperin, T., Fominykh, A., Effect of Solute Concentration Level on the Rate of Coupled Mass and Heat Transfer During Solid Sphere Dissolution in a Uniform Fluid Flow, *Chemical Engineering Science, 56* (2001), 10, pp. 3065-3074

[8]   Waslo, S., Gal-or, B., Boundary Layer Theory for Mass and Heat Transfer in Clouds of Moving Drops, Bubbles or Solid Particles, *Chemical Engineering Science, 26* (1971), 6, pp. 829-838

[9]   Prakash Bharti, R., Chhabra, R. P., Eswaran, V., Effect of Blockage on Heat Transfer from a Cylinder to Power Law Liquids, *Chemical Engineering Science, 62* (2007), 17, pp. 4729-4741

[10]   Mahalingam, R., Chan, S. F., Coulson, J. M., Laminar Pseudoplastic Flow Heat Transfer with Prescribed Wall Heat Flux, *Chemical Engineering J., 9* (1975), 2, pp. 161-166

[11]   Kleinstreuer, C., Wang, T.-Y., Mixed Convection Heat and Surface Mass Transfer between Power-Law Fluids and Rotating Permeable Bodies, *Chemical Engineering Science, 44* (1989), 12, pp. 2987-2994

[12]   White, J. L., Metzner, A. B., Thermodynamic and Heat Transport Considerations for Viscoelastic Fluids, *Chemical Engineering Science, 20* (1965), 12, pp. 1055-1062

[13]   Shenoy, A. V., Mashelkar, R. A., Laminar Natural Convection Heat Transfer to a Viscoelastic Fluid, *Chemical Engineering Science, 33* (1978), 6, pp. 769-776

[14]   Syrjala, S., Laminar Flow of Viscoelastic Fluids in Rectangular Ducts with Heat Transfer: A Finite Element Analysis, *Int. Comm. Heat and Mass Transfer, 25* (1998), 2, pp. 191-204

[15]   Hayat, T., *et al.*, Heat Transfer in Pipe Flow of a Johnson-Segalman Fluid, *Int. Comm. Heat and Mass Transfer, 35* (2008), 10, pp. 1297-1301

[16]   Hammad, K. J., Vradis, G. C., Viscous Dissipation and Heat Transfer in Pulsatile Flows of a Yield-Stress Fluid, *Int. Comm. Heat and Mass Transfer, 23* (1996), 5, pp. 599-612

[17]   Beg, O. A., *et al.*, Computational Fluid Dynamics Modelling of Buoyancy Induced Viscoelastic Flow in a Porous Medium with Magnetic Field, *Int. J. Applied Mechanics Engineering, 6* (2001), 1, pp. 187-210

[18]   Bhargava, R., *et al.*, Numerical Study of Heat Transfer of a Third Grade Viscoelastic Fluid in Non-Darcy Porous Media with Thermophysical Effects, *Physica Scripta*: *Proc. Royal Swedish Academy of Sciences, 77* (2008), pp. 1-11

[19]   Beg, O. A., *et al.*, Computational Modeling of Biomagnetic Micropolar Blood Flow and Heat Transfer in a Two-Dimensional Non-Darcian Porous Medium, *Meccanica, 43* (2008), 4, pp. 391-410

[20]   Zueco, J., Beg, O. A., Network Numerical Simulation Applied to Pulsatile Non-Newtonian Flow through a Channel with Couple Stress and Wall Mass Flux Effects, *Int. J. Applied Mathematics and Mechanics, 5* (2009), 2, pp. 1-16

[21]   Walters, K., Non-Newtonian Effects in Some Elastico-Viscous Liquids whose Behaviour at Small Rates of Shear is Characterized by a General Linear Equation of State, *Quart. J. Mech. Applied. Math., 15* (1962), 1, pp. 63-76

[22]   Soundalgekar, V. M., Puri, P., On Fluctuating Flow of an Elastico-Viscous Fluid Past an Infinite Plate with Variable Suction, *J. Fluid Mechanics, 35* (1969), 3, pp. 561-573

[23]   Rath, R. S., Bastia, S. N., Steady Flow and Heat Transfer in a Visco-Elastic Fluid between Two Coaxial Rotating Disks, *Proc. Mathematical Sciences, 87* (1978), 8, pp. 227-236

[24]   Roy, J. S., Chaudhury, N. K., Heat Transfer by Laminar Flow of an Elastico-Viscous Liquid along a Plane Wall with Periodic Suction, *Czech. J. Physics, 30* (1980), 11, pp. 1199-1209

[25]   Raptis, A. A., Takhar, H. S., Heat Transfer from Flow of an Elastico-Viscous Fluid, *Int. Comm. Heat and Mass Transfer, 16* (1989), 2, pp. 193-197

[26]   Chang, T. B., *et al.*, Numerical Study of Transient Free Convective Mass Transfer in a Walters-B Viscoelastic Flow with Wall Suction, *J. Theoretical Applied Mechanics*, under review (2009)

[27]   Nanousis, N., Unsteady Magnetohydrodynamic Flows in a Rotating Elasto-Viscous Fluid, *Astrophysics and Space Science, 199* (1993), 2, pp. 317-321

[28]   Sharma, V., Rana, G. C., Thermosolutal Instability of Walters' (model B') Visco-Elastic Rotating Fluid Permeated with Suspended Particles and Variable Gravity Field in Porous Medium, *Int. J. Applied Mechanics Engineering, 6* (2001), 4, pp. 843-860

[29]   Sharma, R. C., Kumar, P., Sharma., S., Rayleigh-Taylor Instability of Walter' B' Elastico-Viscous Fluid through Porous Medium, *Int. J. Applied Mechanics Engineering, 7* (2002), 2, pp. 433-444

[30]   Chaudhary, R. C., Jain, P., Hall Effect on MHD Mixed Convection Flow of a Viscoelastic Fluid Past an Infinite Vertical Porous Plate with Mass Transfer and Radiation, *Theoretical and Applied Mechanics, 33* (2006), 4, pp. 281-309

Prasad, V. R., *et al.*: Unsteady Free Convection Heat and Mass Transfer in a …
THERMAL SCIENCE, Year 2011, Vol. 15, Suppl. 2, pp. S291-S305

S305

[31] Ray Mahapatra, T., Dholey, S., Gupta, A. S., Momentum and Heat Transfer in the Magnetohydrodynamic Stagnation-Point Flow of a Viscoelastic Fluid toward a Stretching Surface, *Meccanica, 42* (2007), 3, pp. 263-272

[32] Veena, P. H.,,, Pravin, V. K., Padashetty, S. C., Non-Similar Solutions in Viscoelastic MHD Flow and Heat Transfer over a Porous Stretching Sheet with Internal Heat Generation and Stress Work, *Int. J. Modern Mathematics, 2* (2007), 2, pp. 267-281

[33] Rajagopal, K., Veena, P. H., Pravin, V. K., Nonsimilar Solutions for Heat and Mass Transfer Flow in an Electrically Conducting Viscoelastic Fluid over a Stretching Sheet Saturated in a Porous Medium with Suction/Blowing, *J. Porous Media, 11* (2008), 2, pp. 219-230

[34] Pohlhausen, E., Heat Transfer between Solid Body and Fluid Flow with Small Friction Forces and Small Heat Flux (in German), *ZAMM, 1* (1921), pp. 115-121

[35] Somers, E. V., Theoretical Considerations of Combined Thermal and Mass Transfer from Vertical Flat Plate, *Journal of Appl. Mech., 23* (1956), 295-301

[36] Mathers, W. G., Madden, A. J., Piret, E. L., Simultaneous Heat and Mass Transfer in Free Convection, *Ind Engg. Chem., 49* (1956), 961-968

[37] Gebhart, B., Pera, L., The Nature of Vertical Natural Convection Flows Resulting from the Combined Buoyancy Effects of Thermal and Mass Diffusion, *International Journal of Heat and Mass Transfer, 14* (1971), 12, pp. 2025-2050

[38] Soundalgekar, V. M., Ganesan, P., Finite Difference Analysis of Transient Free Convection with Mass Transfer on an Isothermal Vertical Flat Plate, *International Journal of Engineering Science, 19* (1981), 6, pp. 757-770

[39] Prasad., V. R., Bhaskar Reddy, N., Muthucumaraswamy, R., Radiation Effects on MHD unsteady Free Convection Flow with Mass Transfer Past a Vertical Plate with Variable Surface Temperature and Concentration, *Journal of Energy, Heat and Mass Transfer, 31* (2009), pp. 239-260

[40] Incropera, F. P., Dewitt, D. P., Fundamentals of Heat and Mass Transfer, 5th ed., John Wiley and Sons, New York, USA, 2007

[41] Crank, J., Nicolson, P., A Practical Method for Numerical Evaluation of Solutions of Partial Differential Equations of the Heat Conduction Type, *Proc. Camb. Phil. Society, 43* (1947), pp. 50-67

[42] Prasad, V. R., Bhaskar Reddy, N., Muthucumaraswamy, R., Radiation and Mass Transfer Effects on Two-Dimensional Flow Past an Impulsively Started Infinite Vertical Plate, *Int. J. Thermal Sciences, 46* (2007), 12, pp. 1251-1258

[43] Gebhart, B., *et al.*, Buoyancy-Induced Flows and Transport, Hemisphere, Washington, USA, 1988